

Variability in Diurnal and Seasonal Ambient Conditions on Geothermal Plant Performance and Cost

Dayo Akindipe, Erik Witter, and Matthew Prilliman

National Renewable Energy Laboratory

Keywords

geothermal power cycle; ambient temperature; diurnal and seasonal variability; LCOE

ABSTRACT

Geothermal plant performance is bounded by the second law efficiency, which accounts for the quantity of exergy that can be converted into useful work. This, in turn, is dependent on the geothermal resource temperature and the temperature of the heat sink (i.e., the ambient temperature). In this study, we show that ambient temperature variability on a diurnal and seasonal basis can affect performance and cost estimations for geothermal plants. We have utilized the updated System Advisor Model (SAM) to assess nine geothermal sites with existing resource capacities across three climate zones. Our analysis shows that both evaporatively-cooled flash and air-cooled binary cycle plants are affected by temperature, with a slightly higher effect in enhanced geothermal system binary sites. By assuming an ambient (wet bulb) temperature baseline of 15.6°C (60°F) and comparing baseline results to those from site-specific data, we observe up to 15% underestimation of plant performance and up to 20% overestimation of cost. These results make a case for the inclusion of location-based weather data as inputs to supply curves that are used in capacity expansion models for the prediction of future geothermal deployment scenarios.

1. Introduction

Geothermal energy for electricity generation is a growing market in the United States. With intensifying research, development, and demonstration, and enabling policies around enhanced geothermal systems (EGS) as well as closed-loop and superhot rock technologies, there is an anticipated upsurge in geothermal energy utilization for both electricity generation and direct-use applications (Robins et al., 2021; Augustine et al., 2023). Like all thermo-electric power cycles, the performance of a geothermal power cycle is limited by the first and second laws of thermodynamics. The first law determines how much thermal energy can be extracted from the subsurface. The first law does not account for the interaction of the system with the external environment, which can limit energy conversion reversibility. The second law efficiency accounts for this interaction via the entropy term, and further constrains how much convertible energy (i.e.,

exergy) can be extracted from a geothermal fluid to drive a turbine generator for a given resource temperature and the sink temperature (Mines, 2016). This, in turn, defines the gross plant power output per unit mass flow of produced geothermal fluid, i.e., the brine effectiveness, an important parameter in geothermal plant design. In many thermodynamic and thermoeconomic analyses, the sink temperature of the cycle (i.e., the ambient temperature) is assumed to be a constant. Although this could be valid if a single location is assumed, it does not hold for regional- and national-scale analyses, nor does it account for daily and seasonal changes in ambient temperature. In the western United States, where existing geothermal power plants are situated, ambient temperatures vary diurnally and seasonally due to climatic differences and topography. Ambient temperatures changes have a more pronounced impact on air-cooled power systems than on wet or evaporatively cooled plants.

Previous studies that investigated the effect of ambient temperature dynamics on plant performance have been exergoeconomic studies and power cycle optimization modeling for a single plant and two-plant comparisons (e.g., Michaelides and Michaelides, 2010; Soheli et al., 2011; Kahraman et al., 2019; Pons, 2019; Sukra et al., 2023). Michaelides and Michaelides (2010) performed an exergy analysis of plants running on flash-based cycles. They reported that temperature variations could lead to power output fluctuations between 24% in single-flash and 22% in dual-flash cycles, respectively (Michaelides and Michaelides, 2010). Kahraman et al. (2019) determined from a single-plant (binary cycle) analysis that an ambient temperature increase from 5°C to 35°C causes a 6.8-MW decrease in power generation resulting from a drop (54.9% to 36.7%) in second law efficiency (Kahraman et al., 2019). These studies reveal that ambient temperature variation affects plant performance. However, they do not make comparisons across technologies and multiple sites.

In this work, we use the updated “Geothermal” model in the System Advisor Model (SAM) to determine the effect of diurnal and seasonal variability in ambient temperature on geothermal plant performance and costs. This updated model incorporates the legacy cost and performance calculations in the Microsoft Excel-based Geothermal Electricity Technology Evaluation Model (GETEM) with the unique capabilities of SAM to create a more robust bottom-up model. We apply this model to both flash and air-cooled binary plants driven by geothermal fluids from hydrothermal and EGS resources. We make case study runs for nine locations in California, Nevada, and Oregon for each resource-technology pair within different climate zones in western United States. SAM is used to access the historical multiyear weather data from the National Solar Radiation Database (NSRDB) for each location. The multiyear hourly temperatures are averaged to a single-year time series and then used to calculate the hourly brine effectiveness and generated power. These parameters are used to determine the location-adjusted annual power generation, net capacity factor, capital cost, and levelized cost of electricity (LCOE) for the selected sites. The results derived from this analysis will inform whether location-based weather data needs to be accounted for in the supply (cost versus capacity) curves that are used as inputs to capacity expansion models for the prediction of future geothermal deployment scenarios. This will, in turn, support stakeholders in the decision-making process for future investments in geothermal projects.

2. Methodology

We used SAM, developed by the National Renewable Energy Laboratory (NREL), to perform bottom-up estimations of the system performance and costs for selected geothermal sites. The Geothermal model in SAM has recently undergone significant improvements to better match the outputs from the legacy GETEM used widely by industry. These changes were discussed in a webinar held on January 19, 2023 (<https://sam.nrel.gov/geothermal.html>). In addition, existing capabilities in SAM are being harnessed to further increase the accuracy and representativeness of simulation results. One of these capabilities is the inclusion of ambient weather conditions that affect modeling outcomes. Originally, in the GETEM model, users could only use the default 10°C ambient temperature for binary systems and the 15.6°C (60°F) wet bulb temperature for flash systems. In the next SAM release, users will be able to apply the ambient temperatures from actual weather files in their simulations.

In this work, we used the updated Geothermal model in SAM to determine the effect of diurnal and seasonal variability in ambient temperature on geothermal plant performance and costs. We applied the updated SAM model to both flash and air-cooled binary plants driven by geothermal brine from hydrothermal and near-field EGS resources. To assess this, we have selected nine sites with existing geothermal resource capacity. Table 1 shows the site descriptors including the site number, name, geolocation (i.e., latitude and longitude), resource temperature, depth, and other properties. All sites are located within western United States—California, Nevada, and Oregon—where significant geothermal development has occurred over time.

Table 1. Site Characteristics for the Selected Geothermal Resources in the Western United States

Site Code	Site Name	State	Latitude	Longitude	Köppen Climate Zone	Site Elevation, m	Reservoir Temperature, °C	Reservoir Depth, m	Resource-Technology Pair	Annual Avg. Ambient Temperature, °C	Annual Avg. Wet Bulb Temperature, °C
EM	East Mesa	CA	32.78	-115.25	BWh-Subtropical desert	-19	170	2,000	EGS Binary	23.2	13.8
LVM	Long Valley (Mammoth)	CA	37.64	-118.91	Csb- Warm-summer Mediterranean,	1,258	175	2,000	EGS Binary	6.1	1.4
BM	Blue Mountain	NV	41.00	-118.13	BSk-Mid-latitude steppe	1,258	175	2,000	EGS Binary	10.5	4.7
COSO	Coso Area	CA	36.05	-117.77	BSk-Mid-latitude steppe	1,322	250	2,500	EGS Flash	14.4	6.6
SS	Salton Sea Area	CA	33.20	-115.60	BWh-Subtropical desert	-67	250	2,500	EGS Flash	23.6	14.1
HI	Heber I	CA	32.72	-115.53	BWh-Subtropical desert	0	170	1,219	Hydrothermal Binary	23.3	13.6
HII	Heber II	CA	32.72	-115.53	BWh-Subtropical desert	0	205	1,219	Hydrothermal Flash	23.3	13.6
MHS	Mickey Hot Springs	OR	42.35	-118.35	BSk-Mid-latitude steppe	1,492	170	1,067	Hydrothermal Binary	7.9	3.4
FLV	Fish Lake Valley	NV	37.86	-118.05	BSk-Mid-latitude steppe	1,306	205	1,524	Hydrothermal Flash	14.2	6.5

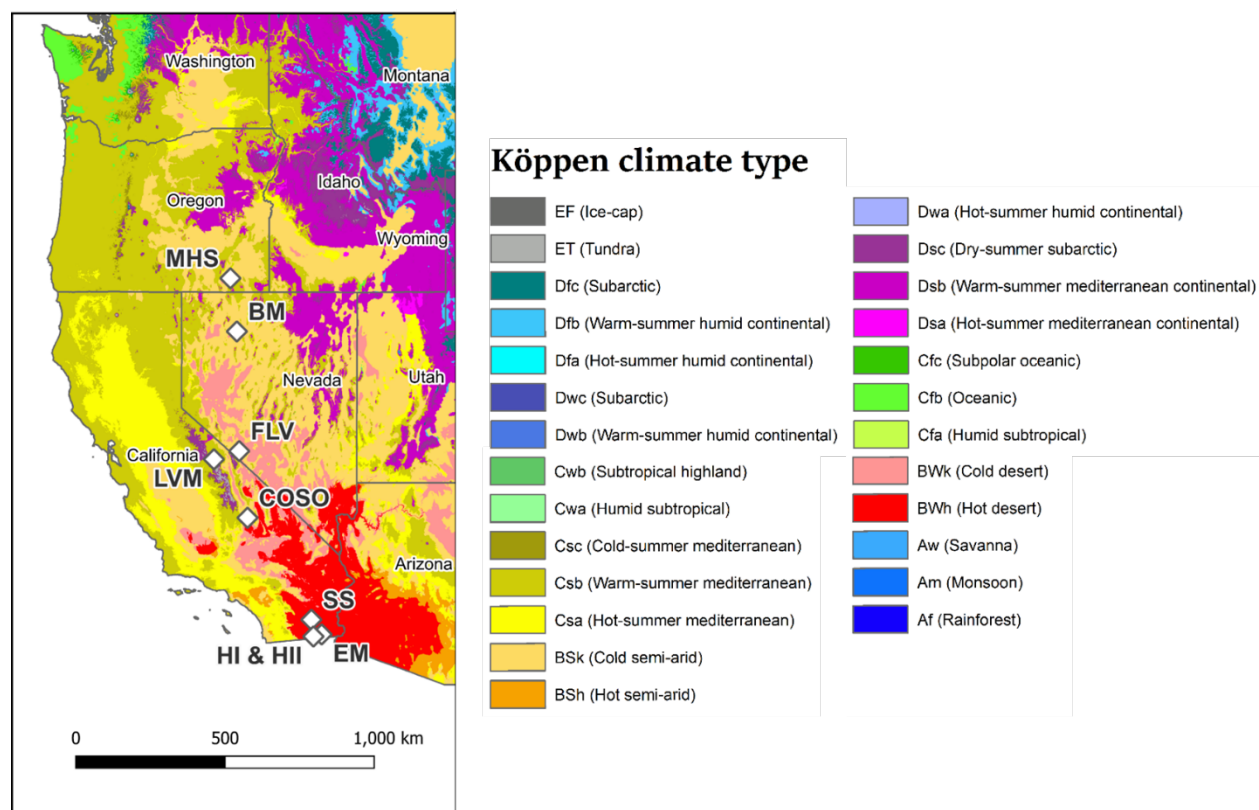


Figure 1: Geospatial map of western U.S. locations of selected sites and their Köppen-Geiger climate zones.

Figure 1 reveals the geolocation of the selected sites on a spatial map of the western United States. The sites cut across three Köppen-Geiger climate zones, including BWh - Subtropical desert, Csb - warm-summer Mediterranean, and BSk - Mid-latitude steppe. Each climate zone is characterized by distinct surface mean temperatures and precipitation patterns that vary diurnally and seasonally during the course of a year. For example, as illustrated in the time series in Figure 2, the hourly temperatures experienced at Salton Sea with a subtropical desert climate (at -67-meter elevation) are on average more than 15°C higher than those in the Mediterranean-climate Long Valley site. Five of the sites have been identified as having resources for both hydrothermal and near-field EGS. Only Fish Lake Valley and Mickey Hot Springs are strictly hydrothermal.

We have classified the surface power blocks as either flash steam cycles or binary cycles. Flash plants typically run on either wet steam or saturated water. During flashing, the inlet geofluid undergoes a pressure drop, which results in a two-phase (steam and saturated water) system. The saturated water at the bottom of the vessel can undergo multiple flash stages to increase the amount of latent heat that can be extracted from the geofluid to drive the turbine. However, practically no more than three flashing stages are implemented in geothermal plants. This is because of a diminishing returns effect of cost versus efficiency gain (Harvey & Wallace, 2016; Fallah et al., 2018). In this work, we compared the performance and cost for single and dual flashing stages. We also applied the flash-to-binary threshold at a resource temperature of 200°C, just as in the

NREL Annual Technology Baseline (NREL, 2023). Therefore, a geothermal (hydrothermal or EGS) resource at a temperature below 200°C is tied to a binary cycle at the surface, while one with a resource temperature at or above this threshold is paired with a flash technology-based steam cycle.

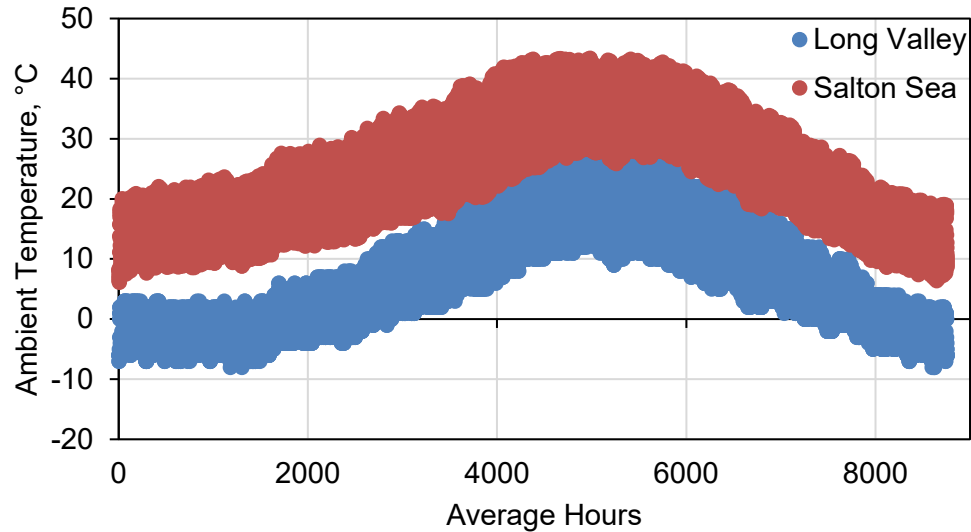


Figure 2: An annual time series showing ambient temperature variation for Long Valley and Salton Sea.

An overview of the methodology applied to this study is shown in Figure 3. As a first step, we used the “Ambient Conditions” module in SAM to download weather files from 1998–2020 from the NSRDB for each site using their latitudes and longitudes. Each weather file (in .CSV file format) contains the ambient (dry bulb) temperature, relative humidity, and dew point, among other variables for each hour in a single year. The multiyear hourly data was averaged to a single-year time series in Excel and then uploaded back into SAM. Examples of ambient temperature time series from the multiyear hourly data are shown in Figure 2. Afterward, the SAM input file was initialized by specifying the input variables for each site. Input variables are categorized as those that define (1) the geothermal resource (e.g., resource temperature, depth, resource potential), (2) plant operations (e.g., net power output/power sales, plant type—flash or binary, geofluid production rate, ambient weather conditions), (3) field installation costs (e.g., number of exploration wells, pump unit cost, drilling success rate), (4) operating cost, and (5) financial parameters (e.g., discount rate, tax rate, depreciation). A list of the input variables and their values can be found in Table 2. The model was then simulated for each site-resource-technology pair. Two simulations were implemented per site-plant technology pairs. The first uses a baseline wet bulb temperature of 15.6°C, while the second simulation uses the site-specific wet bulb temperature calculated from the weather data.

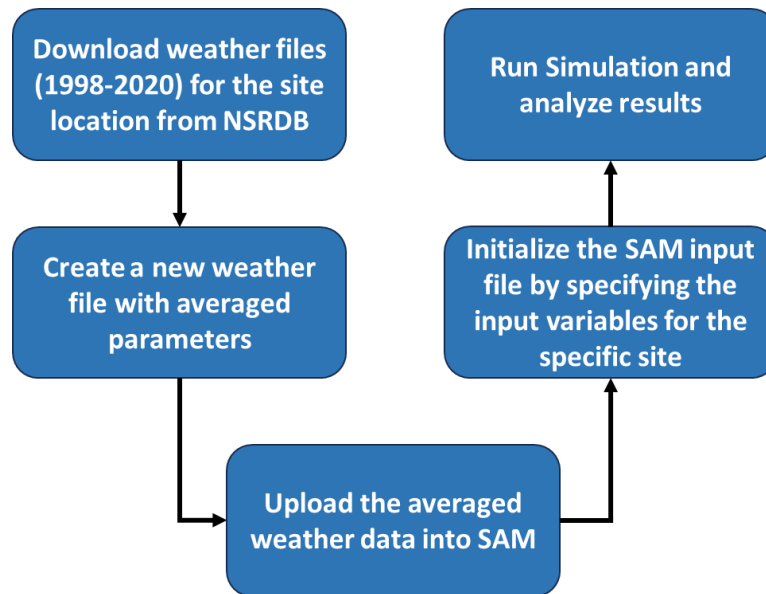


Figure 3: An overview of the methodology applied in this study.

Table 2: Input variables used in the SAM simulations for the four resource and plant technology pairs.

	Hydrothermal		EGS	
Plant technology	Flash	Binary	Flash	Binary
Cooling technology	Evaporative (Wet-cooled)	Air-cooled (Dry-cooled)	Evaporative (Wet-cooled)	Air-cooled (Dry-cooled)
Power output (power sales), MW	30	30	30	30
Production rate per well, kg/s	80	110	40	40
Pressure drawdown, psi/1,000 lb/h	0.4	0.4	4	4
Annual temperature decline	0.5%	0.5%	0.5%	0.5%
Drilling cost curve (U.S. DOE, 2019)	Baseline	Baseline	Baseline	Baseline
Well/Completion type (Lowry et al., 2017)	Vertical - open hole	Horizontal - deviated liner	Vertical - open hole	Horizontal - deviated liner
Well diameter (Lowry et al., 2017)	Small	Large	Small	Large
Number of successful exploration wells	3	3	5	5
Fixed operating cost, \$/kW-yr (NREL, 2023)	113.62	151.06	202.55	452.52
Discount rate (nominal)	7%	7%	7%	7%
Federal income tax rate	20.1%	20.1%	20.1%	20.1%
State income tax rate	7%	7%	7%	7%
Property tax rate (% of total installed cost)	1%	1%	1%	1%
Insurance rate (% of total installed cost)	0.50%	0.50%	0.50%	0.50%

3. Results and Discussion

The results of the SAM runs for each site are shown in Table 3. All sites are compared to a baseline that assumes a constant wet bulb temperature of 15.6°C (i.e., 60°F) as used in the GETEM model. The results reveal that the second law efficiency—defined by the brine effectiveness—is a strong function of the wet bulb temperature for both flash and binary systems. The significance of this effect differs by power cycle type (flash versus binary and single versus dual flash) and location (i.e., climate zone and topography) of the resource. In the following subsections, we discuss the impact of each factor in detail.

Table 3: Results from the SAM simulations for all nine sites.

Site Code	Site Name	Classification	Calculation Type	Brine Effectiveness (w-h/lb)	Pump Work (MW)	Gross Output From (MW)	Net Capital Cost per Watt (\$/kW)	LCOE (\$/MWh)
EM	East Mesa	EGS Binary	Baseline	8.79	37.55	67.55	6023	462
			Actual Site Data	8.93	36.31	66.31	5967	437
LVM	Long Valley (Mammoth)	EGS Binary	Baseline	8.94	36.23	66.23	5962	444
			Actual Site Data	9.86	29.51	59.51	5594	344
BM	Blue Mountain	EGS Binary	Baseline	8.94	36.23	66.23	5962	444
			Actual Site Data	9.66	30.77	60.77	5665	360
COSO	Coso Area	EGS (Single) Flash	Baseline	11.68	13.37	43.37	5062	149
			Actual Site Data	12.77	11.72	41.73	4802	136
		EGS (Dual) Flash	Baseline	13.77	10.32	40.32	4598	128
			Actual Site Data	14.80	9.33	39.33	4425	120
SS	Salton Sea Area	EGS (Single) Flash	Baseline	11.68	13.37	43.37	5062	149
			Actual Site Data	11.86	13.06	43.07	5017	146
		EGS (Dual) Flash	Baseline	13.77	10.32	40.32	4598	128
			Actual Site Data	13.94	10.14	40.14	4568	127
HI	Heber I	Hydrothermal Binary	Baseline	5.97	6.44	36.44	2437	70
			Actual Site Data	6.07	6.32	36.32	2418	69
HII	Heber II	Hydrothermal (Single) Flash	Baseline	6.63	2.18	32.18	2203	50
			Actual Site Data	6.86	2.11	32.11	2170	49
		Hydrothermal (Dual) Flash	Baseline	8.87	1.56	31.56	1939	46
			Actual Site Data	9.09	1.53	31.53	1921	45
MHS	Mickey Hot Springs	Hydrothermal Binary	Baseline	5.90	6.67	36.67	2272	68
			Actual Site Data	6.47	6.04	36.04	2182	64
FLV	Fish Lake Valley	Hydrothermal (Single) Flash	Baseline	6.63	2.24	32.24	2496	54
			Actual Site Data	7.63	1.99	31.99	2342	51
		Hydrothermal (Dual) Flash	Baseline	8.87	1.61	31.61	2180	49
			Actual Site Data	9.84	1.49	31.49	2083	47

3.1 Flash Power Cycle

The results for the sites with flash steam cycles (Table 3) show that the brine effectiveness is better optimized in the dual flash than in the single flash systems. The move from single to dual reduces the parasitic load required for geofluid pumping, thereby decreasing the capital cost and LCOE. The degree of cost reduction is more prominent in EGS flash systems than in hydrothermal flash due to the significant decrease in the number of pumped production wells required for flow and pressure sustenance and heat transfer within the power cycle. Figure 4 compares the performance and cost parameters for the actual temperature data to the baseline inputs for hydrothermal flash sites—Heber II (HII-A and HII-B) and Fish Lake Valley (FLV-A and FLV-B) and EGS flash - Coso (COSO-A and COSO-B) and Salton Sea (SS-A and SS-B). The letters “A” and “B” represent “single” and “dual” flash, respectively. Generally, the percentage difference from the baseline is more prominent in the single flash case than in the dual flash. This suggests that the single flash system is more sensitive to changes in the ambient temperature compared to the dual flash system. By comparing across geothermal resources, it is evident that sensitivities to ambient weather conditions do not vary based on resource type (EGS versus hydrothermal) but on-site location. For example, the Salton Sea EGS flash experienced similar sensitivities to ambient temperature as the Heber II hydrothermal flash.

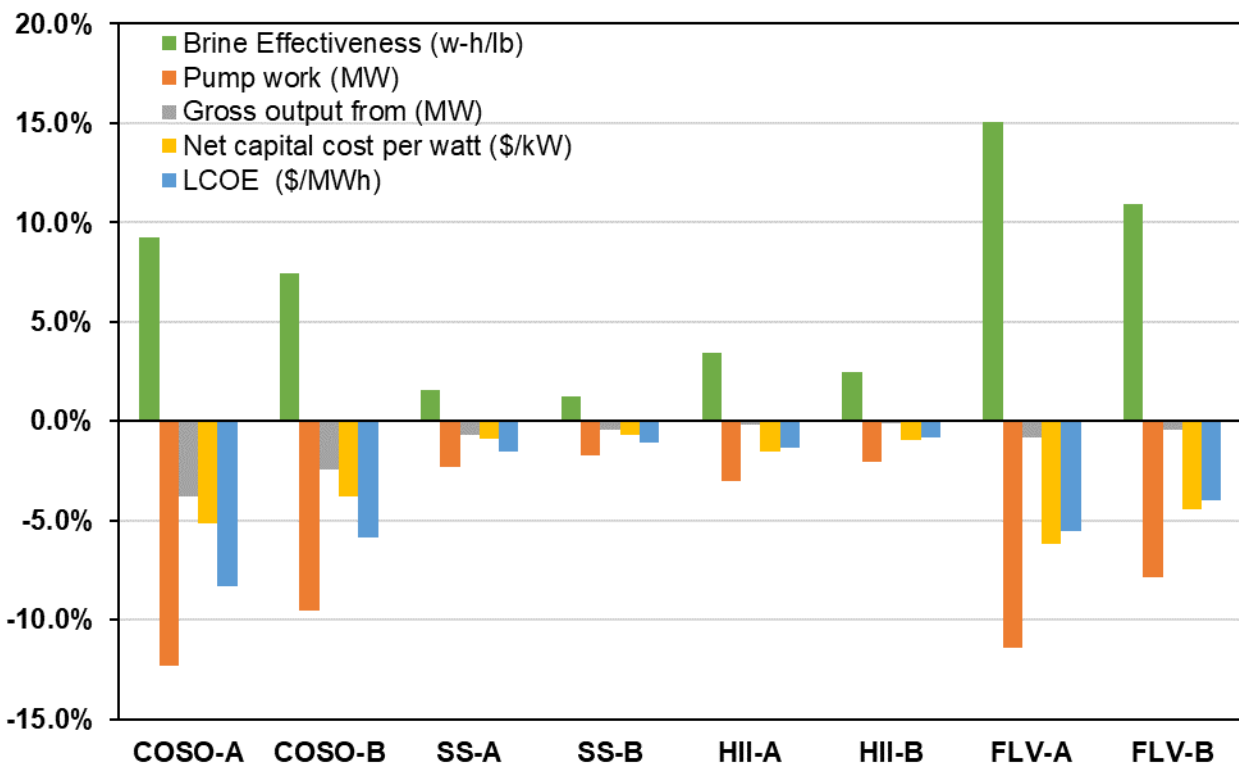


Figure 4: Percentage difference of performance and cost outputs between the baseline and actual data for flash-based power cycles.

3.2 Binary Power Cycle

The majority of binary cycle plants in operation in the United States have an air-cooled condenser system. These condensers operate on the principle of forced convection of ambient air to cool the turbine outlet working fluid. GETEM and SAM assume an air-cooled binary cycle consisting of a turbine generator, an air-cooled condenser, heat exchangers, and working fluid pump. In this study, we have paired lower temperature geothermal resources ($<200^{\circ}\text{C}$) with binary cycles. Hence, the available energy (i.e., exergy), which is a strong function of the reservoir temperature (and the ambient temperature), is less than in the flash case. Therefore, for the same net power output (30 MW), a binary plant will require a higher wellfield flow rate into the heat exchanger unit to maximize conversion (first law) efficiency. On the other hand, higher brine effectiveness (and second law efficiencies) can be achieved compared to flash systems. However, this must be optimized against cost. This is because at high brine effectiveness, the cost of installed plant equipment increases (Mines, 2016). Each SAM simulation is preceded by a binary plant optimization simulation to determine the brine effectiveness that minimizes cost. Therefore, binary systems may be cost-optimized to lower brine effectiveness compared to the unconstrained flash systems. These factors together with significant parasitic pumping requirements cause binary plant costs to be significantly higher than those of flash plants. A typical example is the comparison of Heber I hydrothermal-binary and Heber II hydrothermal-dual flash, at the same location and resource depth, with a baseline LCOE of 70 \$/MWh and 46 \$/MWh, respectively. For the same location, the binary system seems to be characterized by similar levels of sensitivities to changes in ambient temperature compared to the flash system. This is shown in Figure 5, for Heber I hydrothermal-binary (HI) and Heber II hydrothermal-flash (HII-B). Although there is a higher sensitivity on the performance results for flash, there is a corresponding higher sensitivity on LCOE results in the binary case.

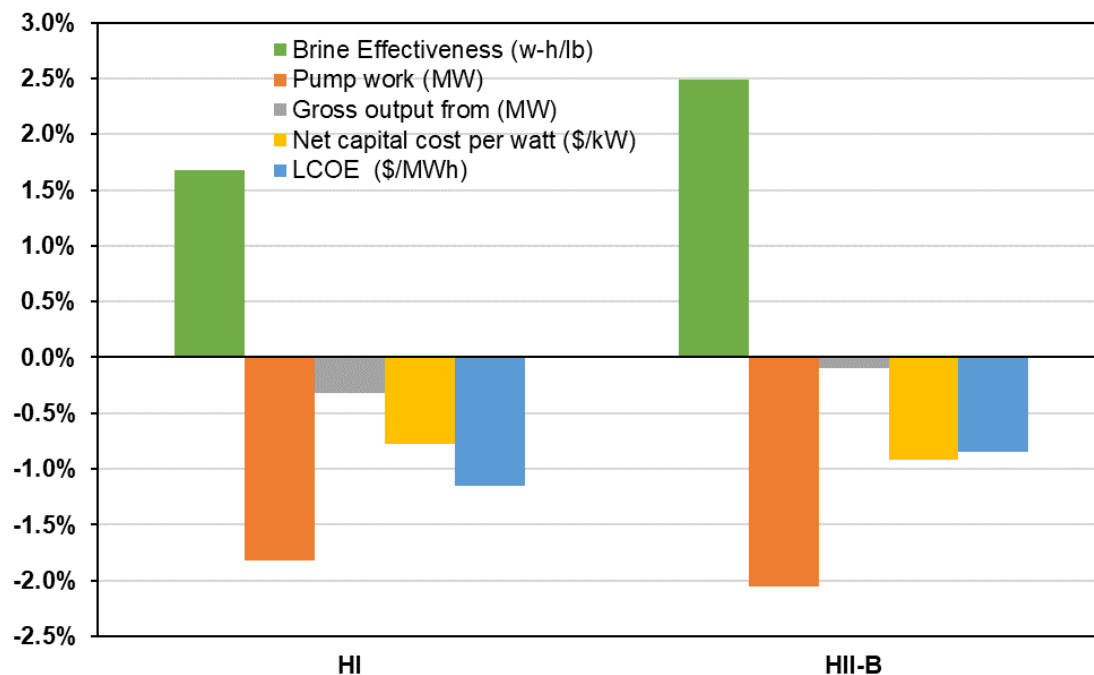


Figure 5: Percentage difference of performance and cost outputs between the baseline and actual data for the Heber I hydrothermal-binary power cycle (HI) and Heber II hydrothermal-dual flash cycle (HII-B).

3.3 Climate Zone Effect

We have established three climate zones among the selected sites: (a) BWh - Subtropical desert, (b) BSk - Mid-latitude steppe, and (c) Csb - Warm-summer Mediterranean. The subtropical desert climate sites are described by high average temperatures ($\sim 23^{\circ}\text{C}$) compared to sites in the other zones. Therefore, coupled with their low relative humidity, the wet bulb temperatures for BWh sites are close to the baseline wet bulb temperature (15.6°C) used in this study. Therefore, as shown in Figure 6, they appear to be less sensitive to the change in the baseline temperature irrespective of resource type or conversion technology. To understand the effect of location and climate zone, we discuss the results for the EGS-binary and hydrothermal-flash cases. For the EGS-binary case, we assess results from the East Mesa (Subtropical desert climate), Long Valley (Warm-summer Mediterranean climate), and Blue Mountain (Mid-latitude steppe climate) sites. These sites are characterized by similar resource temperatures and depth but with varying ambient temperatures. From Table 3, it is evident that the Long Valley site has the least LCOE (344 \$/MWh) compared to Blue Mountain and East Mesa. This is because the Long Valley EGS-binary cycle is characterized by a higher brine effectiveness and less parasitic pumping needed at lower ambient temperatures, resulting in the lowest gross power output among the three sites. Also, as shown in Figure 6, the use of the baseline temperature assumption instead of the actual site data can result in more than 20% overestimation of the LCOE in the Long Valley EGS-binary case. Similar observations are also made for hydrothermal-binary and hydrothermal-flash plants. For example, by looking at Mickey Hot Springs (BSk - Mid-latitude steppe) with a comparable resource temperature and depth as the Heber I site (BWh - Subtropical desert), there is a more significant overestimation of the pump work and LCOE in the former than in the latter. Thus, not accounting for site-specific ambient temperatures and their variability could propagate errors in large-scale models.

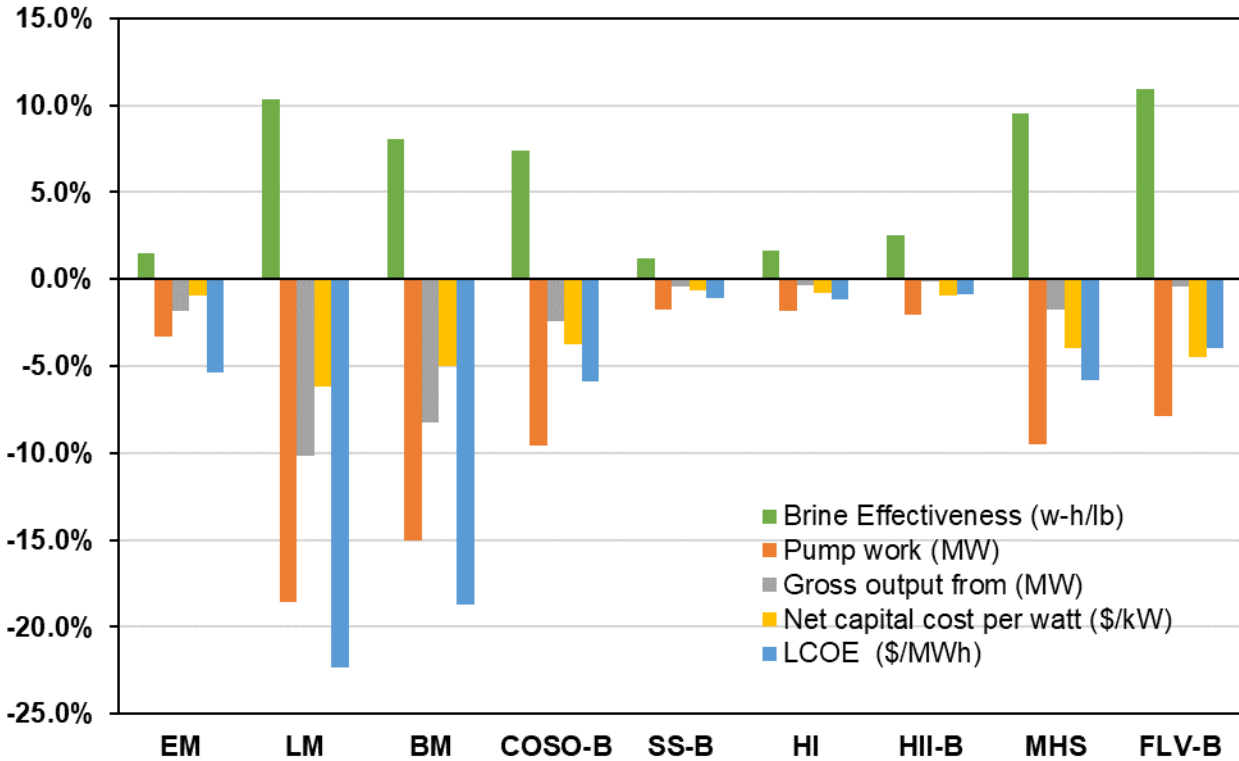


Figure 6: Percentage difference of performance and cost outputs between the baseline and actual data for sites across multiple climate zones.

4. Conclusion

In this study, we assessed the effect of ambient temperature variability on geothermal performance and cost estimations. Nine geothermal sites with existing resource capacities were selected based on type of resource (hydrothermal versus EGS), conversion technology (flash versus binary), geolocation, and climate zone. The results show that temperature variability from a constant baseline wet bulb temperature of 15.6°C typically assumed for geothermal systems can result in close to 15% underestimation of plant performance and up to 20% overestimation of cost, within the context of the case study sites. The severity of this error propagation may be more significant in larger-scale studies. Therefore, it is necessary that future regional and national geothermal cost estimations and projections account for site-specific ambient temperatures and their variability.

Acknowledgement

This work was authored by the National Renewable Energy Laboratory, operated by Alliance for Sustainable Energy, LLC, for the U.S. Department of Energy (DOE) under Contract No. DE-AC36-08GO28308. Funding was provided by the U.S. Department of Energy Office of Energy Efficiency and Renewable Energy (EERE) Geothermal Technologies Office (GTO). The views expressed in the article do not necessarily represent the views of the DOE or the U.S. Government. The U.S. Government retains and the publisher, by accepting the article for publication, acknowledges that the U.S. Government retains a nonexclusive, paid-up, irrevocable, worldwide license to publish or reproduce the published form of this work, or allow others to do so, for U.S. Government purposes.

REFERENCES

- Augustine, C., Fisher, S., Ho, J., Warren, I., & Witter, E. (2023). *Enhanced Geothermal Shot Analysis for the Geothermal Technologies Office* (NREL/TP-5700-84822). National Renewable Energy Laboratory. <https://doi.org/10.2172/1922621>
- Fallah, M., Ghiasi, R. A., & Mokarram, N. H. (2018). A comprehensive comparison among different types of geothermal plants from exergy and thermoeconomic points of view. *Thermal Science and Engineering Progress*, 5, 15–24. <https://doi.org/10.1016/j.tsep.2017.10.017>
- Harvey, W., & Wallace, K. (2016). 10 - Flash steam geothermal energy conversion systems: Single-, double-, and triple-flash and combined-cycle plants. In R. DiPippo (Ed.), *Geothermal Power Generation* (pp. 249–290). Woodhead Publishing. <https://doi.org/10.1016/B978-0-08-100337-4.00010-3>
- Kahraman, M., Olcay, A. B., & Sorgüven, E. (2019). Thermodynamic and thermoeconomic analysis of a 21 MW binary type air-cooled geothermal power plant and determination of the effect of ambient temperature variation on the plant performance. *Energy Conversion and Management*, 192, 308–320. <https://doi.org/10.1016/j.enconman.2019.04.036>
- Lowry, T. S., Finger, J. T., Carrigan, C. R., Foris, A., Kennedy, M. B., Corbet, T. F., Doughty, C. A., Pye, S., & Sonnenthal, E. L. (2017). *GeoVision Analysis: Reservoir Maintenance and Development Task Force Report (GeoVision Analysis Supporting Task Force Report : Reservoir Maintenance and Development)* (SAND2017-9977). Sandia National Lab. (SNL-NM), Albuquerque, NM (United States). <https://doi.org/10.2172/1394062>
- Michaelides, E. E., & Michaelides, D. N. (2010). The effect of ambient temperature fluctuation on the performance of geothermal power plants. *International Journal of Exergy*. <https://www.inderscienceonline.com/doi/10.1504/IJEX.2011.037216>
- Mines, G. (2016). 13 - Binary geothermal energy conversion systems: Basic Rankine, dual-pressure, and dual-fluid cycles. In R. DiPippo (Ed.), *Geothermal Power Generation* (pp. 353–389). Woodhead Publishing. <https://doi.org/10.1016/B978-0-08-100337-4.00013-9>
- NREL. (2023). *Geothermal*. Annual Technology Baseline. <https://atb.nrel.gov/electricity/2023/geothermal>

- Pons, M. (2019). Exergy Analysis and Process Optimization with Variable Environment Temperature. *Energies*, 12(24), 24. <https://doi.org/10.3390/en12244655>
- Robins, J., Kolker, A., Flores-Espino, F., Pettitt, W., Schmidt, B., Beckers, K. F., Pauling, H., & Anderson, B. (2021). *2021 U.S. Geothermal Power Production and District Heating Market Report* (NREL/TP-5700-78291). National Renewable Energy Laboratory. <https://dx.doi.org/10.2172/1808679>
- Sohel, M. I., Sellier, M., Brackney, L. J., & Krumdieck, S. (2011). An iterative method for modelling the air-cooled organic Rankine cycle geothermal power plant. *International Journal of Energy Research*, 35(5), 436–448. <https://doi.org/10.1002/er.1706>
- Sukra, K. F. A., Permana, D., & Adriansyah, W. (2023). Modelling and Simulation of Existing Geothermal Power Plant: A Case Study of Darajat Geothermal Power Plant. *International Journal of Thermodynamics*, 26(2), 2. <https://doi.org/10.5541/ijot.1118778>
- U.S. DOE. (2019). *GeoVision: Harnessing the Heat Beneath Our Feet* (DOE/EE–1306). U.S. Department of Energy. <https://www.energy.gov/sites/default/files/2019/06/f63/GeoVision-full-report-opt.pdf>